Supplementary Information

Synthesis and characterization of a new energetic metal-organic framework for use in potentially propellant composition

Shuo Wu‡[a], Min Li‡[a], Zhengyi Yang [a], Zhengqiang Xia[a], Bin Liu[a], Qi Yang*[a], Qing Wei[a], Gang Xie[a], Sanping Chen*[a], Shengli Gao, Jack Y. Lu*[a, b]

Table of Contents

The concept of oxygen balance

The oxygen balance (OB or OB%) is one of the important property of energetic materials. It can be defined as the amount of oxygen remaining after the oxidation of hydrogen, carbon and metal to produce water, carbon dioxide and metal oxide. If excess of oxygen remains after the oxidation reaction, explosive is said to have a positive OB. On the other hand, if the oxygen is completely consumed and excess fuel remains, explosive is said to have a negative OB. Thus, OB values can be positive or negative. However, if an explosive molecule contains just enough oxygen to convert all its carbon to carbon dioxide, all its hydrogen to water and all its metal to metal oxide with no excess, the explosive is said to have a zero OB, but explosives are rarely perfectly balanced. In other words, OB is an expression that is used to indicate the degree to which an explosive can be oxidized.[1]

High nitrogen content in the organic linkers has been a target for the synthesis of EMOFs, and this can increase the oxygen balance relative to conventional carbon-rich linkers. In addition, in order to synthesize more powerful EMOFs with high nitrogen/oxygen contents, different functional groups can be attached to the molecule's backbone. The most interesting functional groups with respect to increasing the oxygen content are nitro, nitrato and nitramine groups, etc.[2]

The oxygen balance of some common energetic materials are as follows:[1]

- 2,4,6-Trinitrotoluene (TNT): −74.00%
- 1,3,5,7-tetranitro-1,3,5,7-tetraazacyclooctane (HMX): −21.68%
- 1,3,5-trinitro-1,3,5-triazinane (RDX): −21.60%
- Ammonium nitrate (AN): +20.00%
- Ammonium dinitramide(ADN): +25.80%
- Ammonium perchlorate (AP): +34.04%

References

1. G. Singh. Recent advances on energetic material. Nova Science Publishers, New York. 2015.
2. K. A. McDonald, S. Seth and A. J. Matzger, Crystal Growth & Design, 2015, 15. 5963-5972.

Fitted equations of magnetism

(1) The $^4T_{1g}$ state of Co^{2+}, the best fits above 30 K was fitted based on the following equation:

$$x = \lambda / kT$$

$$\chi_{Co} = \frac{N\beta^2}{k(T-\theta)x} \frac{\begin{array}{c} \dfrac{7(3-A)^2 x}{5} + \dfrac{12(A+2)^2}{25A} + \left\{ \dfrac{2(11-2A)^2 x}{45} + \dfrac{176(A+2)^2}{675A} \right\} \exp(-5Ax/2) \\ + \left\{ \dfrac{(A+5)^2 x}{9} - \dfrac{20(A+2)^2}{27A} \right\} x \exp(-4Ax) \end{array}}{3 + 2\exp(-5Ax/2) + \exp(-4Ax)}$$

where A is a crystal field parameter (A = 1.5 and 1 in the weak and strong crystal-field limits), k represents electron delocalization (k = 1.0 is minimal), λ is the spin-orbit coupling constant (λ = -176 cm^{-1} is the free-ion value).

(2) The data were fitted using the simple phenomenological equation:

$$\chi T = A\exp(-E_1/kT) + B\exp(-E_2/kT)$$

where the sum of A and B parameters equals the Curie constant, while E_1 and E_2 stand for the "activation energies" of spin–orbit coupling (or site distortion) and antiferromagnetic exchange interactions, respectively.

References

1. J. W. Raebiger, J. L. Manson, R. D. Sommer, U. Geiser, A. L. Rheingold and J. S. Miller, *Inorg. Chem.*, 2001, **40**, 2578-2581.
2. J. M. Rueff, N. Masciocchi, P. Rabu, A. Sironi and A. Skoulios, *Eur. J. Inorg. Chem.*, 2001, 2843-2848.
3. P. Rabu, J. M. Rueff, Z. L. Huang, S. Angelov, J. Souletie and M. Drillon, *Polyhedron*, 2001, **20**, 1677-1685.

Table S1. Some representative azoles and azines compounds and their chemical structures

Azoles		Azines	
Name	Structure	Name	Structure
5-amine-1*H*-1,2,4-triazole	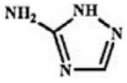	2,4,6-triazido-1,3,5-triazine	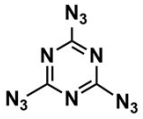
3-amine-5-nitro-2*H*-1,2,4-triazole	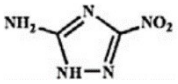	3-amino-6-nitro-1,2,4,5-tetrazine	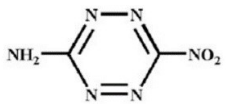
3-(tetrazol-5-yl)triazole	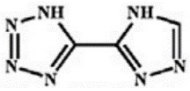	3-amino-6-(3,5-diamino-1H-1,2,4-triazol-1-yl)-1,2,4,5,-tetrazine	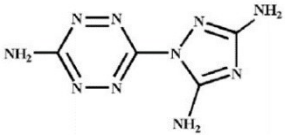
5-(5-amine-1*H*-1,2,4-triazol-3-yl)-3-nitro-1*H*-1,2,4-triazole	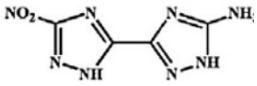	3-(1*H*-1,2,3,4-tetrazol-5-ylamino	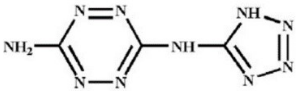
Bis(1*H*-tetrazol-5-yl)amine	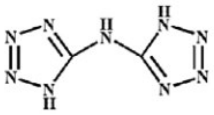	4,4',6,6'-tetra(hydrazino)hydrazo-1,3,5-triazine	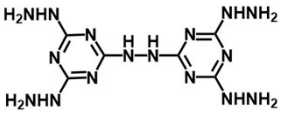
4,5-bis(1*H*-tetrazole)-1*H*-imidazole	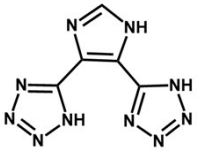	6-((6-amino-1,2,4,5-tetrazin-3-yl)diazinyl)-1,2,4,5-tetrazin-3-amine	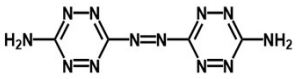
5,5'-(1,2-phenylene)bis(1H-tetrazole)	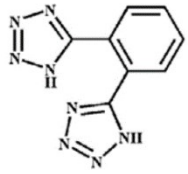	2,5,8-tri(azido)-s-heptazine	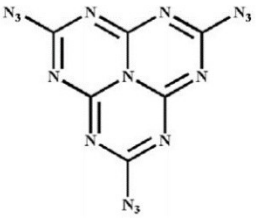

Table S2. The detailed characterization of H_3TATT and $[Co(HTATT)]_n$

	H_3TATT	$[Co(HTATT)]_n$
Formula weight	330.23	386.19
Color	White	Orange
State	Powder	Block crystal
Decomposition temperature	296.6 ℃	342.7 ℃
Solubility	Soluble in DMF and DMSO	Soluble in THF

Table S3. Crystal data and structure refinement details for $[Co(HTATT)]_n$*.

Crystal	$[Co(HTATT)]_n$
Empirical formula	$CoC_6H_3N_{18}$
CCDC number	1864071
Formula weight	386.19
Crystal system	Monoclinic
Space group	$P2_1/c$
a/ Å	8.616(4)
b/ Å	8.888(4)
c/ Å	17.715(8)
α/°	90
β/°	96.499(9)
γ/°	90
V/ Å^3	1347.9(10)
Z	4
$\rho_{calc.}$/g·cm^{-3}	1.903
μ/mm^{-1}	1.316
F(000)	1131.0
GOOF on F^2	0.999
R_1/wR_2 [$I>2\sigma(I)$]	0.0530/0.1249
R_1/wR_2 [all data]	0.1007/0.1496

* $R_1 = \Sigma\left||F_0|-|F_c|\right| / \Sigma|F_0|$, $wR_2 = [\Sigma(F_o^2 - F_c^2) / \Sigma w(F_0)^2]^{1/2}$

Table S4. Bond lengths for $[Co(HTATT)]_n$.

$[Co(HTATT)]_n$	Atom	Atom	Length/Å	Atom	Atom	Length/Å
	Co1	N8	2.016(4)	Co1	N10	2.042(4)
	Co1	N6#1	2.160(5)	Co1	N13#2	2.187(5)
	Co1	N18#3	2.268(4)	Co1	N1	2.288(4)
	N6	Co1#4	2.160(5)	N13	Co1#5	2.187(5)
	N18	Co1#6	2.268(4)			

#1 -X,1/2+Y,1/2-Z; #2 1-X,-1/2+Y,1/2-Z; #3 +X,3/2-Y,-1/2+Z; #4 -X,-1/2+Y,1/2-Z; #5 1-X,1/2+Y,1/2-Z; #6 +X,3/2-Y,1/2+Z

Table S5. Bond lengths for $[Co(HTATT)]_n$.

$[Co(HTATT)]_n$	Atom	Atom	Atom	Angle/°	Atom	Atom	Atom	Angle/°
	N8	Co1	N10	174.49(17)	N8	Co1	N6#1	90.73(18)
	N10	Co1	N6#1	90.26(18)	N8	Co1	N13#2	86.73(17)
	N10	Co1	N13#2	91.76(18)	N6#1	Co1	N13#2	173.98(15)
	N8	Co1	N18#3	95.90(16)	N10	Co1	N18#3	89.38(16)
	N6#1	Co1	N18#3	96.27(17)	N13#2	Co1	N18#3	89.42(16)
	N8	Co1	N1	87.88(16)	N10	Co1	N1	86.96(16)
	N6#1	Co1	N1	80.01(16)	N13#2	Co1	N1	94.44(16)
	N18#3	Co1	N1	174.76(15)	C1	N1	Co1	123.9(4)
	C2	N1	Co1	121.9(3)	N7	N6	Co1#4	126.7(3)
	N5	N6	Co1#4	121.7(3)	C4	N8	Co1	125.9(4)
	N7	N8	Co1	128.2(3)	C5	N10	Co1	127.3(3)
	N11	N10	Co1	127.4(3)	C5	N13	Co1#5	135.1(4)
	N12	N13	Co1#5	118.2(3)	C6	N18	Co1#6	133.0(4)

N17	N18	Co1#6	118.6(3)

#1 -X,1/2+Y,1/2-Z; #2 1-X,-1/2+Y,1/2-Z; #3 +X,3/2-Y,-1/2+Z; #4 -X,-1/2+Y,1/2-Z; #5 1-X,1/2+Y,1/2-Z; #6 +X,3/2-Y,1/2+Z

Table S6. Hydrogen bond lengths (Å) and angles(°) for $[Co(HTATT)]_n$.

$[Co(HTATT)]_n$	D-H···A	d(D-H)/Å	d(H-A)/Å	d(D-A)/Å	D-H-A/°
	N(4)-H(4)···N(3)	0.86	2.55	3.311(7)	149
	N(9)-H(9) ···N(11)	0.86	2.08	2.932(7)	172
	N(14)-H(14) ···N(5)	0.86	1.82	2.681(8)	176

Table S7. The thermokinetics parameters of the exothermic process of $[Co(HTATT)]_n$ at four different heating rates.

Heating rate β (°C min^{-1})	Peaks temperatures T_p (°C)
2	353.8
5	363.4
8	370.4
10	374.7
E_k (kJ mol^{-1})	251.402
lnA_k (s^{-1})	42.321
E_o (kJ mol^{-1})	249.142

Table S8. Calculated parameters used in the detonation reaction for $[Co(HTATT)]_n$.

	EMOF (hartree)	Co (hartree)	NH_3 (hartree)	C (hartree)	N_2 (hartree)	ΔE_{det} (hartree)	ΔE_{det} (kcalg^{-1})	ΔH_{det} (kcalg^{-1})
$[Co(HTATT)]_n$	-1360.5342	-145.008	-56.505	-37.738	-109.448	2.2852	3.7131	4.2307

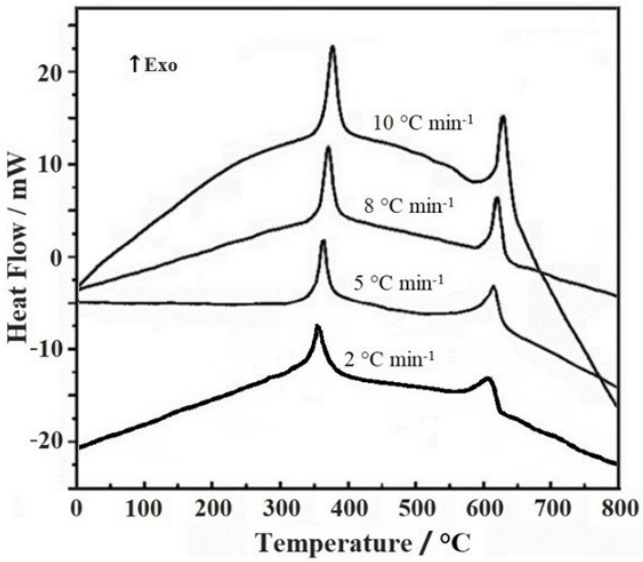

Figure S1. DSC curves of $[Co(HTATT)]_n$ at four different heating rates of 2, 5, 8, and 10 °C min^{-1}.

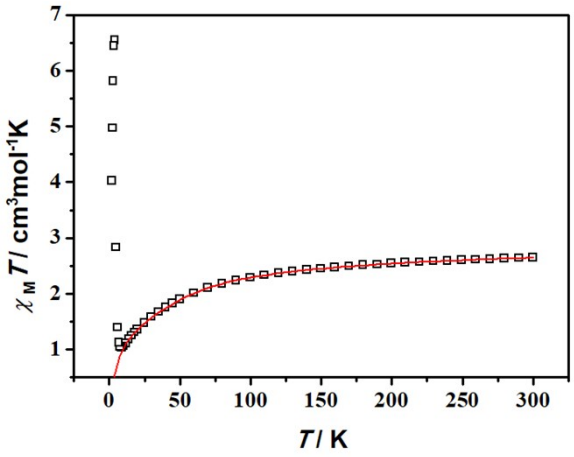

Figure S2. The fits of the data accounting to the spin-orbit coupling λ for the $^4T_{1g}$ state of Co(II) ion.

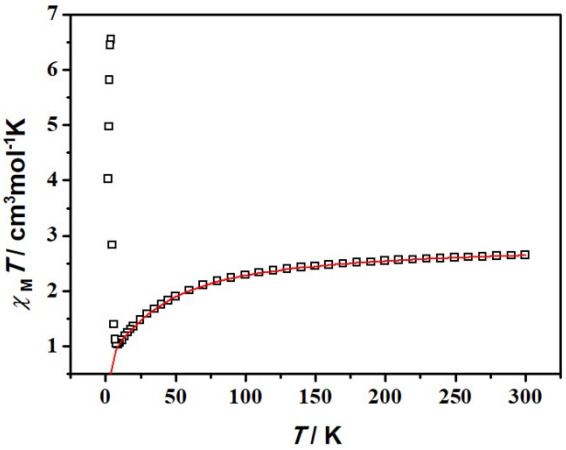

Figure S3. The fits of the data using the simple phenomenological equation.